

Effect on an Outpost of Lunar Vehicle Impact and Debris

Kristina D. Zaleski* and Robert H. Tolson†

North Carolina State University, Raleigh, NC, 27695

NASA's current exploration plans call for a permanent base on the moon. After the establishment of a lunar outpost, resupply missions will be required to ferry humans and supplies to the outpost. Of concern is the situation where propulsion is lost during the lunar descent phase. The Instantaneous Impact Point (IIP) is the location a lunar lander would impact if it lost propulsion and followed a ballistic trajectory. The lander's trajectory must be constrained to ensure the IIP is sufficiently far from the outpost. This ensures that dust and debris ejected in an impact are not sent in the direction of the outpost.

Nomenclature

<i>ALHAT</i>	Autonomous Landing and Hazard Avoidance Technology
<i>ALSEP</i>	Apollo Lunar Surface Experiment Package
<i>CEV</i>	Crew Exploration Vehicle
<i>IIP</i>	Instantaneous Impact Point
<i>LM</i>	Lunar Module

I. Introduction

President Bush, in his Vision for Space Exploration, has announced that we should establish an outpost on the surface of the moon.

Using the Crew Exploration Vehicle, we will undertake extended human missions to the moon as early as 2015, with the goal of living and working there for increasingly extended periods.

The establishment of an outpost will create new concerns that were not faced during the Apollo missions to the moon. One major concern is debris and ejecta that is created during a landing. Apollo 12 returned to the landing site of Surveyor 3, a robotic precursor to the Apollo missions. Apollo 12 landed only 155 m from Surveyor with a terminal velocity of 15 ft/s in the vertical direction, and no velocity component in the horizontal direction.¹ Surveyor's television camera arm was brought back to Earth to be studied. Many micro-craters were found on the surface of Surveyor. Most interestingly, one side of the arm had 100 times as many impacts as the rest of the arm, with impact craters as big as 300 micrometers.¹ Analysis of the landing site configuration showed that the side of the Surveyor camera arm with the most damage was the side that faced the Apollo 12 LM. Thus, one nominal landing of the Apollo LM caused damage to the surface assets. With future lunar missions and the establishment of an outpost, landings at the same location will be frequent, with resupply and astronaut transfer missions, so damage of this type will be recurring. Also, there is the potential for a off-nominal landing, where the lander impacts the surface with a higher velocity.

Another hazard that will need to be assessed for long duration and multiple landing lunar missions is the affect of lunar dust on solar arrays. Katzan and Edwards studied the build-up of dust during multiple nominal landings. They found that after three landings, dust levels 500 m away from the landing site would be $3 \mu\text{m}/\text{cm}^2$. At this level, less than 60% of the light is transmitted through the dust layer to the solar

*Graduate Student, Mechanical and Aerospace Engineering, Student Member

†Langley Professor, Mechanical and Aerospace Engineering, Associate Member

array.² This study looked only at the dust levels that would be created from a nominal landing. If the vehicle was in an abort situation and impacted the surface with a greater than nominal velocity, there is the potential for more dust to accumulate on solar arrays.

Factors that affect impact dynamics are the vehicle mass, speed, geometry, and angle of impact. The higher the energy at impact, $E = 1/2mv^2$, the more lunar debris there will be. Shim, et. al., simulated cratering of vehicles of different geometries, but with the same mass, at low impact speeds (2-4 m/s). Wedge shapes create more debris in the target surface, whereas blocks and cylinders crush more material beneath the vehicle and less debris is ejected.³ Impact tests were performed using the JSC Hypervelocity Impact Test Facility on various shields to determine the survivability of different shields. They found that non-spherical objects would penetrate deeper into the shields than similar mass spheres and the same velocity.⁴

The Instantaneous Impact Point (IIP) is the point that the vehicle would impact the surface if an abort was declared during the descent phase of the mission. The impact velocity, mass, and angle are dependent on when the abort was declared. Debris from the impact will continue in the direction of travel just before the impact. This paper controls the impact by two methods. The first it to always constrain the impact to be downrange of the nominal landing site and surface assets, so that the debris does not travel toward the landing site. This is impossible to do if the trajectory is also constrained to give the astronauts a window view of the landing site during approach. The second method of controlling the impact location by flying at out of plane maneuver so that the IIP never coincides with the nominal landing site. Flying out of plane is done in two ways: controlling the thruster angles during the final landing burn and a inclination change during the deorbit maneuver.

A. Impacts on Moon

There have been many meteor impacts on the surface of the moon. Meteors are solid masses, impacting at high velocities. There have not been many low velocity impacts, similar to what would be caused by a lunar lander with a failed propulsion system. Low velocity impacts of the moon were created by the Ranger missions, Apollo S-IV booster, and Apollo LM's.

The Ranger missions were the first American missions to the moon. The Ranger spacecraft were outfitted with cameras and placed on a trajectory to impact the moon, taking pictures until the spacecraft crashed. From these missions, images were obtained of the lunar surface. However, good impact data was not obtained, because the only observatories of the impact were located back on Earth. Later lunar survey missions, such as Clementine, would survey craters that could possibly have been formed by Ranger impacts. Since it is unknown what impact led to a specific crater, it is not possible to draw a correlation between lunar impact speed and lunar crater diameter.

Apollo missions delivered a seismograph as part of the ALSEP experiment. After the lunar module (LM) returned to the command module, the LM was ejected and placed on a trajectory such that it would impact the surface. If the seismograph was properly working, it should be able to register the LM impact, and it did. This was done with LM's from Apollo 12, 14, and 15.⁵ Since the command module was still in orbit, the approximate location of the impact is known and a correlation can be made between cratering event and crater size.

B. Impacts on Earth

Earth impacts are abundant and so knowledge can be gained regarding crater dynamics. Scaling Earth impacts to model lunar impacts is difficult. The biggest cause for a difference in impact behavior is the moon's lack of an atmosphere and a different gravity field. Both of these things would cause debris to travel further on the moon, given the same initial conditions. However, many crater events have occurred on Earth so it is worth looking at Earth impacts and comparing to the small subset of known lunar impacts.

1. Missile Impacts at White Sands

In the early 1960's, missiles were impacted at the White Sands facility in New Mexico to study crater impact dynamics. Figure 1 shows the ejecta distribution for a crater caused by a missile impact with impact energy of 15.7×10^{14} ergs and an impact angle of 45.9° . The resulting crater was 9.26 m in diameter and 1.98 m deep. The measured displaced ejecta mass was 7,380 kg.

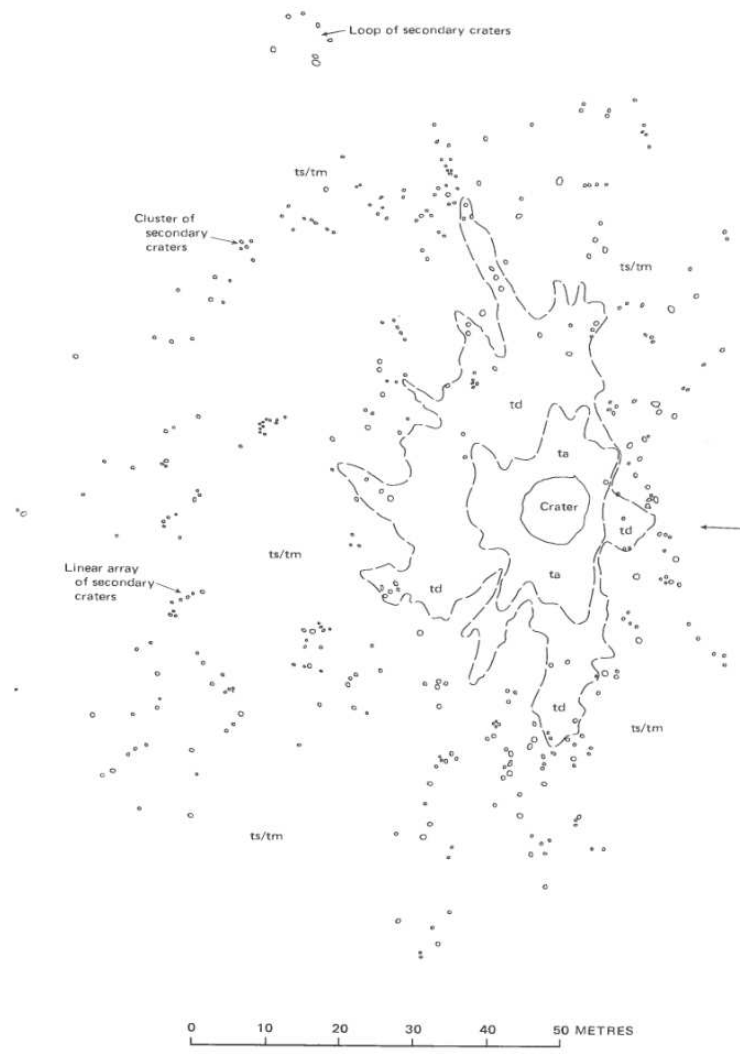


Figure 1. Map of White Sands 15.7×10^{14} ergs missile impact crater showing the distribution of thin to thick ejecta and secondary impact craters.⁶

Figure 2 shows the ejecta distribution for a missile impact with energy of 22.7×10^{14} ergs and an impact angle of 30° . The impact caused a crater diameter of 30.9 feet and 6.5 feet deep. The total mass of ejecta from the impact was 56,300 kg. The impact energy and angle are similar to the impact which caused the crater in Figure 1. The target material for the crater in Figure 2 was soaked with water, which caused a larger crater and more ejecta mass than the similar impact into dry sand.

Figure 3 is a picture taken of one of the craters caused by the missile impact. The arrow shows the direction of travel for the missile. The ejecta can be seen in the image.

There are some characteristic of Earth impacts that will apply to lunar impacts. If the impact occurs with a significant forward velocity (impact is not vertical), then a significant amount of ejecta will travel in the same direction as the vehicle prior to impact.

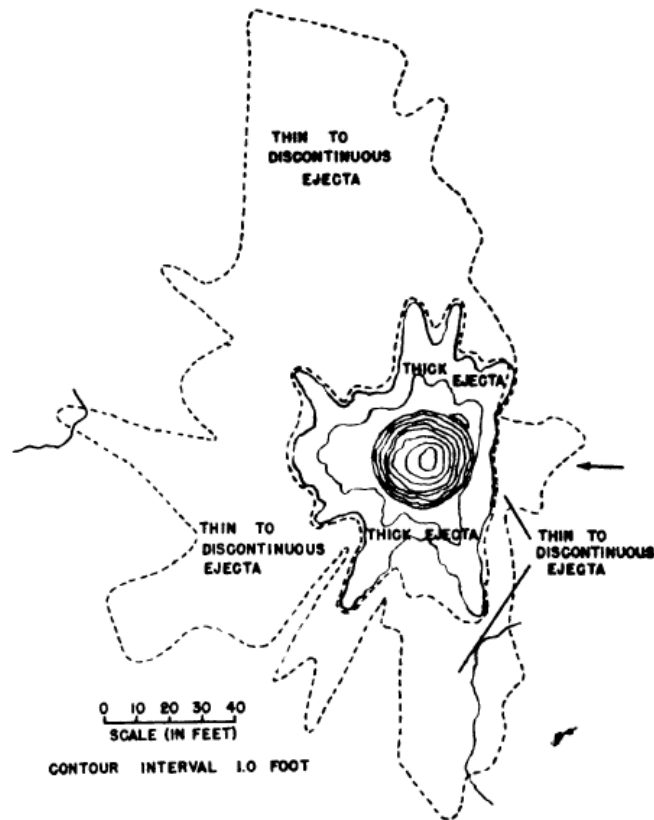


Figure 2. Crater caused by a 22.7×10^{14} ergs missile impact at White Sands.

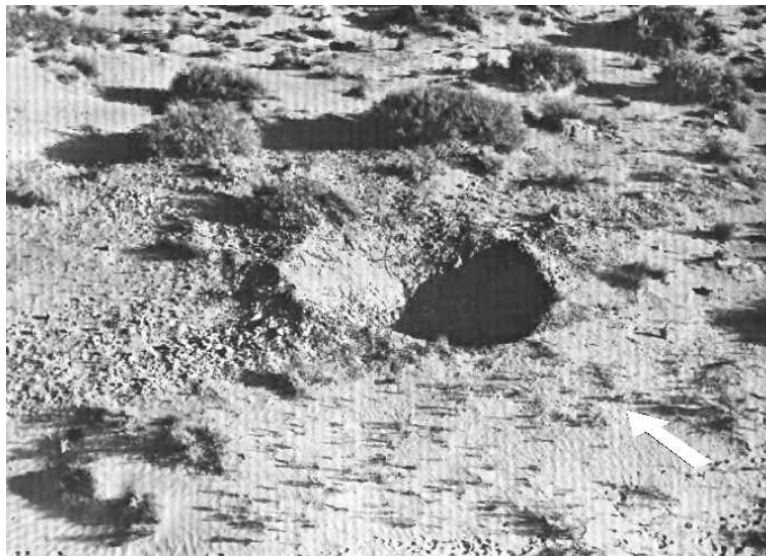


Figure 3. Image of impact crater at White Sands showing the ejecta from the impact. The arrow shows the direction the missile was traveling.

2. Ries Crater

The Ries crater is located in southern Germany, on Earth and in an atmosphere. It is believed to have been created by a meteor impact. Moldavites (green glass debris common to meteor impact events) has

been found in northern Europe. Artemieva, et. al.⁷ are working to model the ejecta field from this impact. Figure 4 shows the moldavite distribution throughout Europe. Figure 5 shows the model⁸ of the ejecta field in two dimensions. From their model, the impact speed of the 200 m diameter meteor was determined to be 10 km/s at an impact angle of 45°, which produced a crater of 1.5-3 km in diameter. Figure 6 shows how the debris may have traveled in time.⁹ This model shows how the debris traveled, not only in the direction of travel, but also out of plane.

The Ries crater event occurred on Earth, under terrestrial gravity and atmosphere, but the general ejecta field can be expected to be the same on the moon. Most of the debris will continue in the direction of travel. A small percentage of the debris will travel back downrange. Other than a fan in the direction of travel, side lobes are not seen in this model.

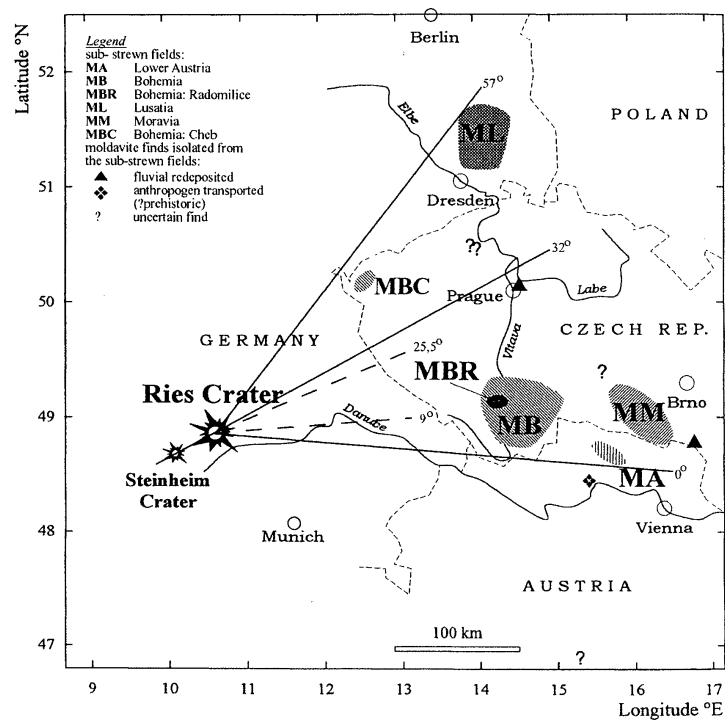


Figure 4. Map of the location of Ries crater and the location of ejecta from the impact.⁷

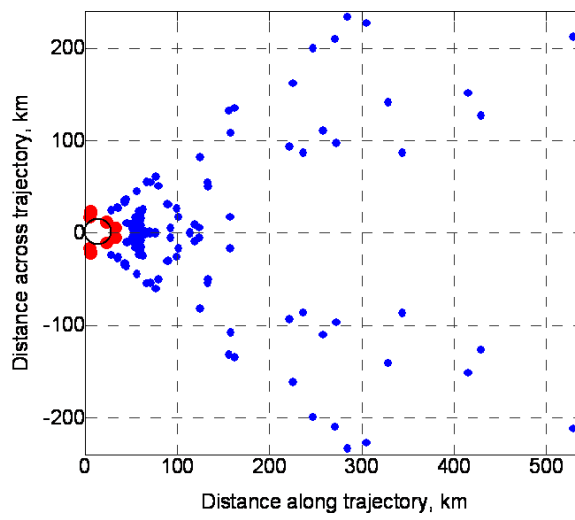


Figure 5. Model of the ejecta fan for the Ries crater event.⁸

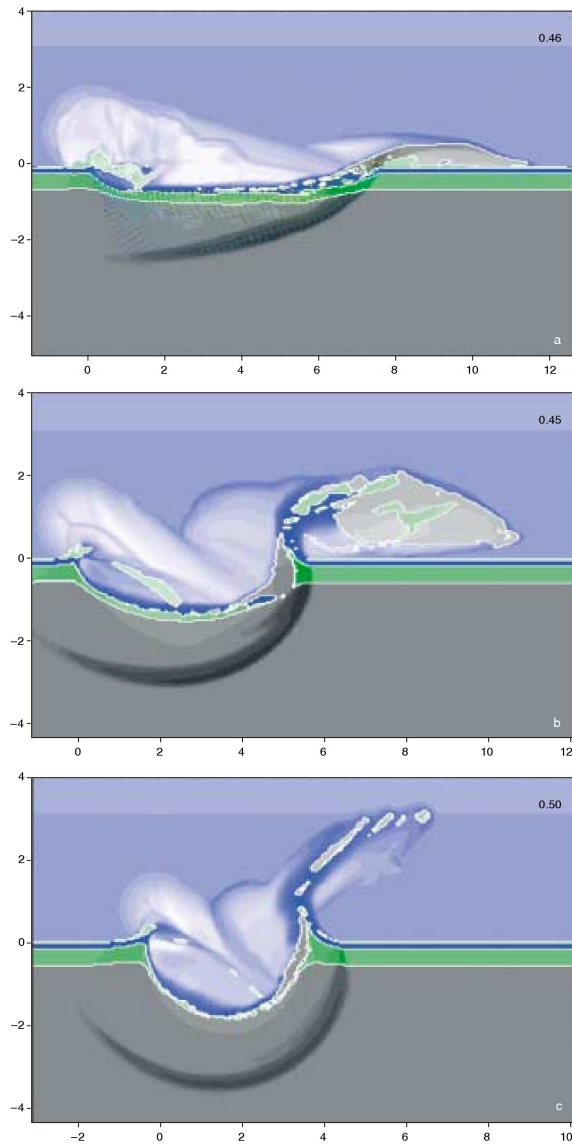


Figure 6. Computer simulation of the formation of Ries crater.¹⁰

C. Impacts on Venus

Imaging of the surface of Venus shows craters with parabolic shaped ejecta fields. Research on the ejecta distribution on Venus includes the affect of the atmosphere on the ballistically traveling ejecta particles.¹¹ Atmospheric affects can be neglected on the moon. What is interesting about the Venusian craters is that the ejecta field is very parabolic in shape. Most of the ejecta continues in the direction of travel, but the parabolic models also include ejecta that traveled in the opposite direction in addition to cross-range. Figure 7 and Figure 8 show two Venusian craters that have ejecta distribution fields which are very parabolic in shape.

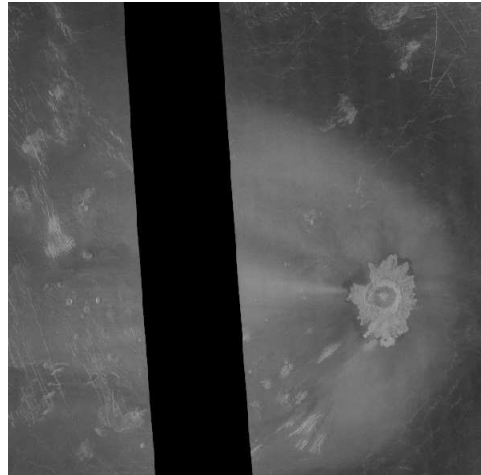


Figure 7. Magellan image of the crater Adivar on Venus.

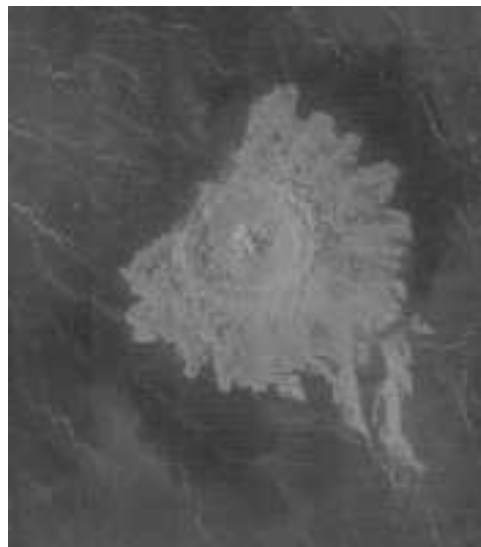


Figure 8. Magellan image of the crater Aurelia on Venus.

II. Downrange Constained Impact

For the nominal lunar descent scenario, the vehicle begins in lunar orbit attached to the Crew Exploration Vehicle (CEV). After separation, the vehicle performs a deorbit maneuver to put it on a 100 km by 15.24 km elliptic orbit. At some optimal point on this orbit, the lander engines come on and burn continuously. The engines can be throttled and positioned in any direction.

To avoid having to address the problem of ejecta from an impact hitting the landing site, the trajectory can be constrained to always have an impact point that is downrange of the landing site. Since most of the ejecta continues in the direction of travel, a downrange impact will have most of the ejecta traveling away from the landing site. This control is done by controlling the engine throttle settings.

Other constraints which are on the trajectory are the final conditions. At an altitude of 30 m, the vehicle should descend at less than 1 m/s and all velocity should be in the vertical direction. The vehicle should do this with a minimum ΔV .

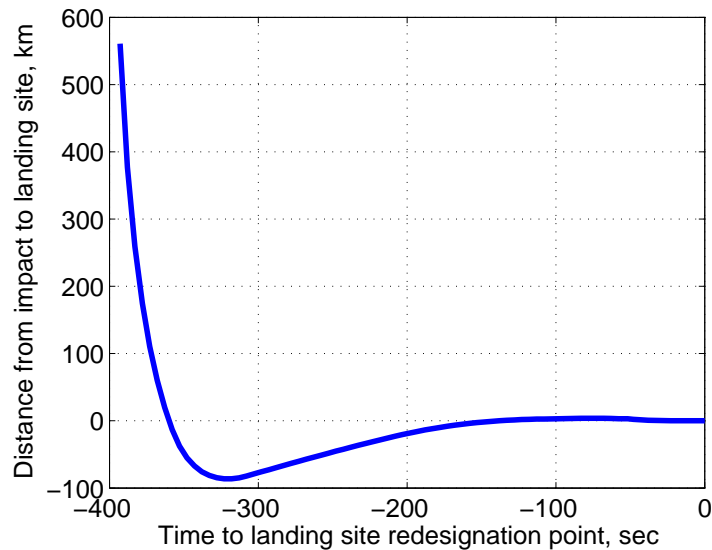


Figure 9. Instantaneous impact point as a function of time.

Figure 9 shows the IIP movement in time. Initially, the IIP is far downrange from the landing site. Downrange is defined to be a positive distance number, whereas uprange is negative. As time progresses and the vehicle slows down, the IIP moves closer to the landing site. At some point, the IIP coincides with the landing site and then continues to move uprange. Eventually, the IIP crosses the landing site again and the IIP becomes the landing site.

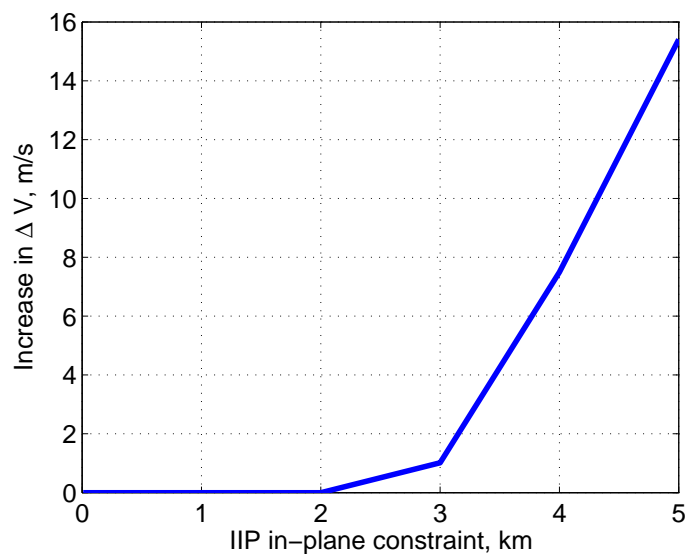


Figure 10. Amount of ΔV that it will cost to constrain the impacts to be always downrange.

III. Constant Stay Out Zone

Constraining the instantaneous impact point to always be downrange of the landing site is not always possible. If the vehicle is required to fly a constant glideslope, it may be difficult or impossible to keep the IIP downrange depending on the shallowness of the glideslope and the length of time that the vehicle must be on the glideslope.

To give the astronauts a view of the landing site out of the window during the final descent, the vehicle should fly a constant glideslope - the rate of change of altitude and flight path angle are held constant. Hazard detection sensors, like ALHAT, work best when the final descent is vertical.¹² Apollo flew a 16° glideslope for 120 seconds.¹³ The study here looks at trajectories with 16°, 45°, and 60° glideslopes for 100 seconds.

Since it is not possible to constrain these three glideslope trajectories to have impacts that are always downrange, the trajectories were perturbed to have out-of-plane impacts when the IIP path crosses over the nominal landing site. This was done using two different methods. The first was to control the out of plane perturbation using the thruster angles during the final descent. The second method was to make an inclination change during the deorbit maneuver.

A. Control with Thruster Angles

Figure 11 shows the location of the impacts. The along track plane was defined as the plane containing the position vectors at the engine ignition and the landing site. The cross track direction is 90° from that plane. The nominal case is always in plane, so the impact path crosses directly over the landing site. The braking thruster angles are used to create an out of plane crossing. This was done for distances from 200 m up to 1 km from the landing site. All of the trajectories come about 1.5 km uprange of the landing site, but do not cross directly over the landing site. Instead, potential impact points occur out of plane.

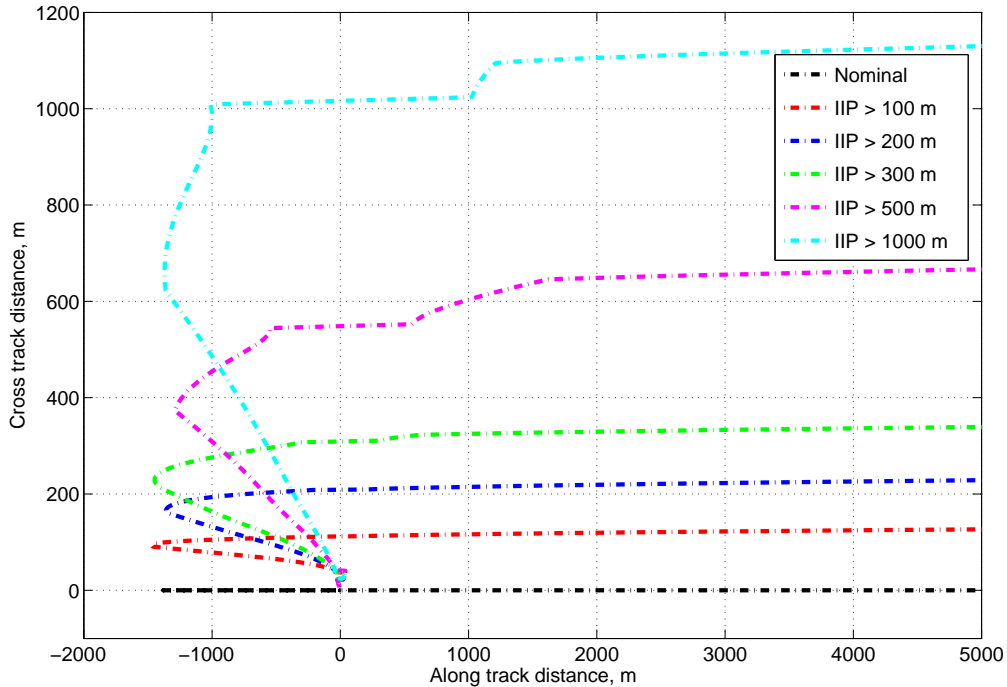


Figure 11. Impact groundtrack for trajectories with various cross range constraints.

The ΔV cost for doing this out of plane maneuver are shown in Figure 12. It would cost less than 10 m/s to divert 1 km out of plane.

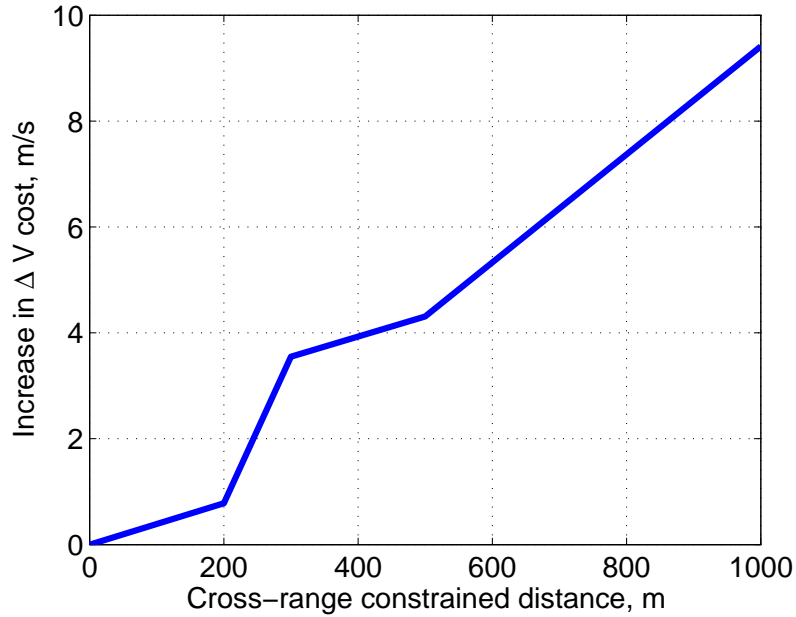


Figure 12. Increase in ΔV cost for out of plane maneuver done with varying the thruster angles during final descent.

B. Control with Deorbit Plane Change

NEED TO FINISH THIS RESEARCH

IV. Impact Crater Sizing

Moore, et. al. studied missile impacts at White Sands and found that the crater diameter was proportional to the energy of the impact. Figure 13 shows the model from their study. Figure 14 shows data from their study, as well as data compiled from lunar impacts. Even though the impacting surface was different, there is a clear trend that can be used to predict the size of future craters. Eq (1) is the empirical model from the missile and lunar impact data.

$$d = 0.0008(mv^2 \sin^2 \theta)^{0.3927} \quad (1)$$

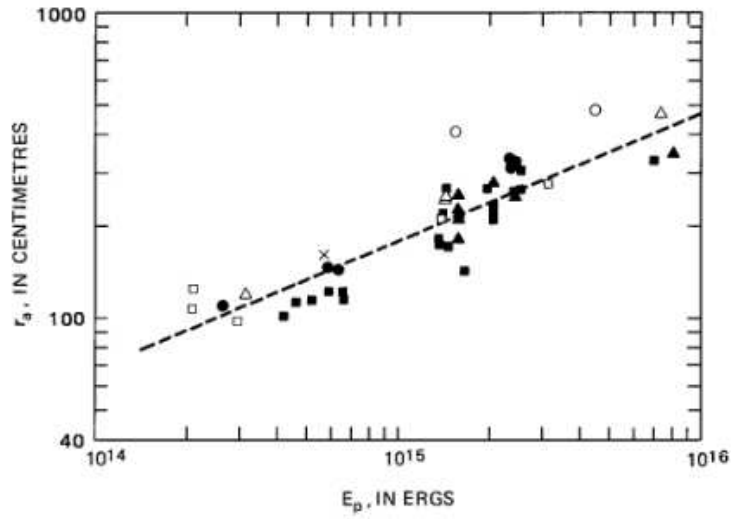


Figure 13. Relationship between impact energy and crater diameter using missile impact data as computed by Moore, et. al.⁶

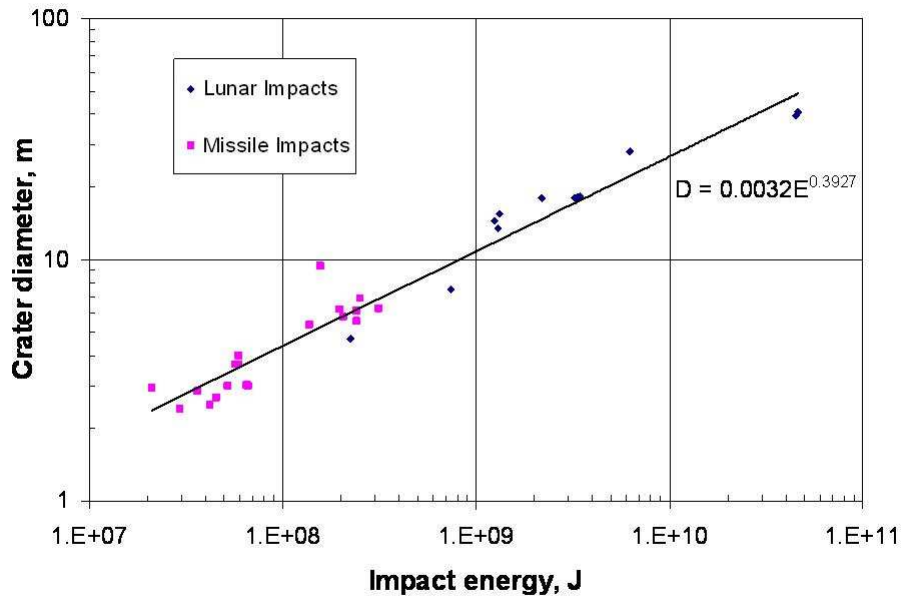


Figure 14. Missile impacts at White Sands and lunar spacecraft impacts.

V. Uniform Ejecta Distribution

Housen, et. al.¹⁴ have derived a set of scaling laws that can be used to determine the ejecta blanket for an impact crater. Their equation for ejecta thickness is shown in Eq. (2),

$$B^* = \frac{A(e_r - 2)}{2\pi} (\sin 2\theta)^{e_r - 2} r^{* - e_r} \left(1 + \frac{4e_r - 5}{3} \left(\frac{r^*}{\sin 2\theta} \right)^{-(e_r - 2)/2} \frac{D}{r^*} \right) \quad (2)$$

where θ is the impact angle, R is the impact crater radius, r is the distance from the crater rim to the point of interest. The expressions e_r , e_x , B^* , and r^* and given in Eq (3)-(6).

$$e_r = \frac{6 + \alpha}{3 - \alpha} \quad (3)$$

$$e_x = \frac{3 - \alpha}{2\alpha} \quad (4)$$

$$B^* = \frac{B}{R} \quad (5)$$

$$r^* = \frac{r}{R} \quad (6)$$

$$(7)$$

Constants A and D were derived empirically by Housen¹⁴ to be $A = 0.32$ and $D = 0.83$.

Eq (2) was used to calculate the ejecta distribution for three different trajectories. Each trajectory has a different glideslope, which affects the amount of braking that was done to slow the vehicle. Figure 15 shows the ejecta distribution for three different glideslopes. The data plotted corresponds to the time that the vehicle crosses over the landing site.

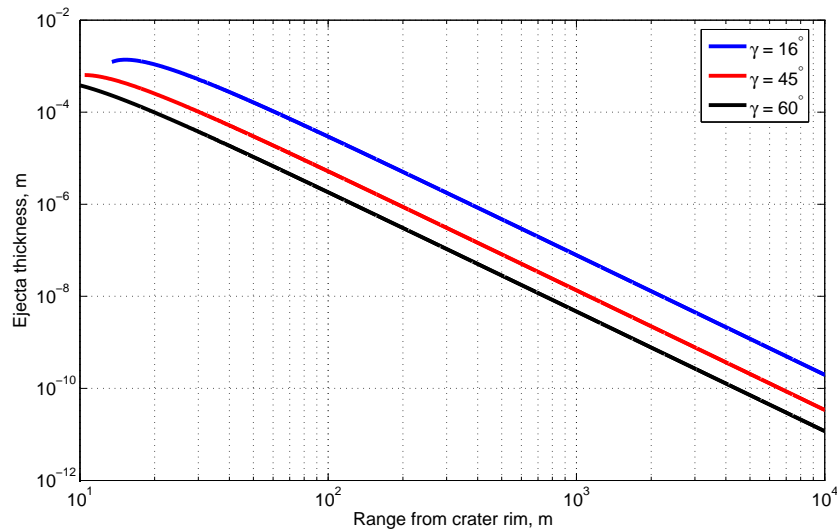


Figure 15. Distribution of ejecta thickness as a function of distance from the impact crater rim, shown for three different glideslope trajectories.

Figure 16 shows the distance from the impact location where the ejecta thickness will be 0.1 mm. If this distance is less than the distance to the nominal landing site, then the ejecta level at the landing site is less. Figure 17 shows the distance from the impact to where the ejecta thickness 1 μm . Forcing the dust levels to be lower causes the distance to be higher.

The dashed lines are the places where the ejecta from the impact will cover the landing site. This is with the assumption that the ejecta distribution is uniform in all directions - it does not matter if the impact occurs uprange or downrange of the landing site. The parts of the trajectory inside of the two dashed lines are the problematic regions that should be avoided.

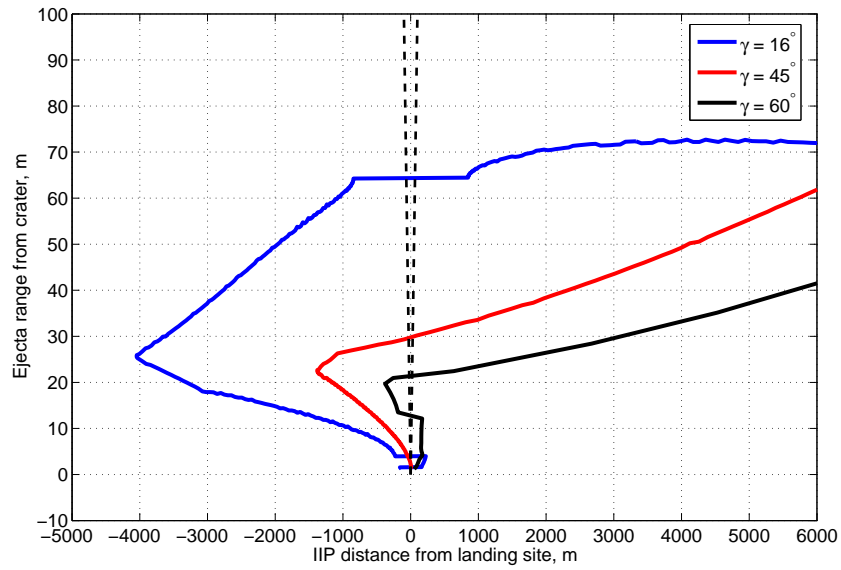


Figure 16. Distance where the ejecta thickness is 0.1mm as a function of impact distance to the landing site.

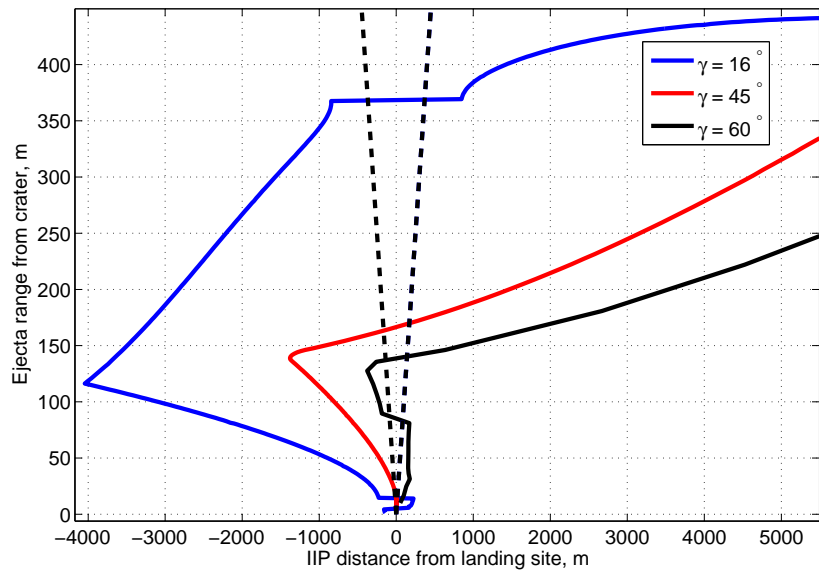


Figure 17. Distance where the ejecta thickness is 1 μm as a function of impact distance to the landing site.

VI. Conclusion

After much typing, the paper can now conclude.

Acknowledgments

A place to recognize others.

References

- ¹ Apollo 12 press release, November 1969. Publication 69-148.
- ² Cynthia Katzan and Jonathan Edwards. Lunar dust transport and potential interactions with power system components. Technical Report NAS3-25266, National Air and Space Administration, November 1991.
- ³ V.P.W. Shim, Z.H. Tu, and C.T. Lim. Two-dimensional response of crushable polyurethane foam to low velocity impact. *International Journal of Impact Engineering*, 24:703–731, 2000.
- ⁴ Eric L. Christiansen and Justin H. Kerr. Projectile shape effects on shielding performance at 7 km/s and 11 km/s. *International Journal of Impact Engineering*, 20:165–172, 1997.
- ⁵ Apollo 16 preliminary science report. Technical Report SP-315, NASA Manned Spaceflight Center, 1972.
- ⁶ H.J. Mores. *Missile Impact Craters (White Sands Missile Range, New Mexico) and Applications to Lunar Research*. Contributions to Astrogeology. US Geological Survey, 1976.
- ⁷ Dieter Stoffer, Natalia Artemieva, and Elisabetta Pierazzo. Modeling the ries-stainheim impact event and the formation of the moldavite strewn field. *Meteoritics and Planetary Science*, 37:1893–1907, 2002.
- ⁸ Impact Cratering: Bridging the Gap Between Modeling and Observations. *Oblique Impact and its Ejecta: Numerical Modeling*, number LPI-1155, 2003.
- ⁹ Natalia Artemieva, Elisabetta Pierazzo, and Dieter Stoffer. Numerical modeling of tektite origin in oblique impacts: Implication to ries-moldavites strewn field. *Bulletin of the Czech Geological Survey*, 77(4):303–311, 2002.
- ¹⁰ 1st International Conference on Impact Cratering in the Solar System. *Numerical Modeling of Impact Cratering*, number SP-612, 2006.
- ¹¹ A.T. Basilevsky, J.W. Head, and A.M. Abdrakhimov. Impact crater air fall deposits on the surface of venus: Areal distribution, estimated thickness, recognition in surface panoramas, and implications of provenance of sampled surface materials. *Journal of Geophysical Research*, 109, 2004.
- ¹² T. Brady and J. Schwartz. Alhat system architecture and operational concept. In *IEEE Aerospace Conference*, pages 1–13, March 2007.
- ¹³ Richard W. Orloff. *Apollo by the numbers: A Statistical Reference*. National Air and Space Administration, 2000.
- ¹⁴ K.R. Housen, R.M. Schmidt, and K.A. Holsapple. Crater ejecta scaling laws: Fundamental forms based on dimensional analysis. *Journal of Geophysical Research*, 88(B3):2485–2499, 1983.